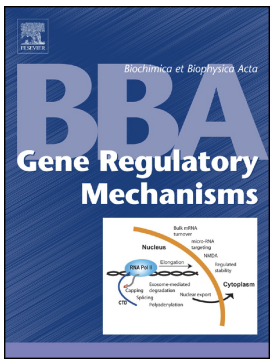

Radiation induced transcriptional and post-transcriptional regulation of the hsa-miR-23a~27a~24–2 cluster suppresses apoptosis by stabilizing XIAP

Theresa Heider, Lisa Mutschelknaus, Vanja Radulović, Klaudia Winkler, Julia Kimmel, Nataša Anastasov, Michael J. Atkinson, Simone Moertl

PII: S1874-9399(17)30128-1
DOI: doi: 10.1016/j.bbagrm.2017.08.006
Reference: BBAGRM 1177

To appear in:

Received date: 24 April 2017
Revised date: 1 August 2017
Accepted date: 21 August 2017

Please cite this article as: Theresa Heider, Lisa Mutschelknaus, Vanja Radulović, Klaudia Winkler, Julia Kimmel, Nataša Anastasov, Michael J. Atkinson, Simone Moertl , Radiation induced transcriptional and post-transcriptional regulation of the hsa-miR-23a~27a~24–2 cluster suppresses apoptosis by stabilizing XIAP, (2017), doi: 10.1016/j.bbagrm.2017.08.006

Radiation induced transcriptional and post-transcriptional regulation of the hsa-miR-23a~27a~24-2 cluster suppresses apoptosis by stabilizing XIAP

Theresa Heider[1], Lisa Mutschelknaus[1], Vanja Radulović[1], Klaudia Winkler[1], Julia Kimmel[1], Nataša Anastasov[1], Michael J. Atkinson[2], Simone Moertl[1]

[1] Helmholtz Center Munich, German Research Center for Environmental Health, Institute of Radiation Biology, Neuherberg, Germany; [2] Chair of Radiation Biology, Technical University Munich, Munich, Germany;

Correspondence:

Dr. Simone Moertl

Helmholtz Center Munich, German Research Center for Environmental Health, Institute of Radiation Biology, Ingolstaedter Landstrasse 1, 85764 Neuherberg, Germany;

E-mail: moertl@helmholtz-muenchen.de; Tel.: +49 (0)89 3187 3143;

Fax: +49 (0)89 3187 3378

Abstract

The non-coding transcriptome, in particular microRNAs (miRNA), influences cellular survival after irradiation. However, the underlying mechanisms of radiation-induced miRNA expression changes and consequently target expression changes are poorly understood.

In this study, we show that ionizing radiation decreases expression of the miR-23a~27a~24-2 cluster through transcriptional regulation by promoter methylation and at the post-transcriptional level by reduced processing through AGO-phosphorylation. Furthermore, we demonstrate that all three mature cluster miRNAs reduce apoptosis by increasing expression of the common target protein XIAP.

These findings link a temporal succession of transcriptional and post-transcriptional regulatory mechanisms of the miR~23a~24-2~27a cluster, enabling a dynamic stress response and assuring cellular survival after radiation exposure.

Key words:

microRNA, stress response, methylation, promoter, AGO, phosphorylation

1. Introduction

microRNAs are highly conserved, small noncoding RNA molecules that negatively regulate gene expression, either by RNA destabilization or by repression of translation [1, 2]. A number of miRNAs are encoded in gene clusters wherefrom they are transcribed into common primary transcripts. Surprisingly, disparate expression patterns for the individual mature miRNAs of a common transcript may occur [3, 4]. In line with individual expression patterns only a few studies report miRNA clusters that co-target the same genes or molecular pathways [5-7].

Radiation-induced expression changes in miRNAs have been described in several human cell types, such as normal human cells [8-10], cancer cells [11-13], as well as in human tissue and blood samples [14-16]. These studies reveal a broad spectrum of radiation-regulated miRNAs, with little overlap between different tissues, suggesting that the radiation response of miRNAs may be specific for cell type, radiation dose and time point. The miRNA response may have an impact in radiotherapy since they are involved in processes important for cellular radiation responses, including DNA damage repair, apoptosis and the activation of signalling cascades [17-19].

The microRNAs miR-23a, miR-27a and miR-24-2 are encoded by an intergenic cluster located on chromosome 19 with a promoter spanning from -603 to +36 relative to the transcription initiation site (+1) [20, 21]. It is transcribed by polymerase II into a common primary (pri) transcript and is further processed into individual mature miRNAs (Fig. 1A I) [20]. Uncommonly the miR-23a~27a~24-2 cluster has an intronic paralog on chromosome 9 (miR-23b~27b~24-1) (Fig. 1A II) [22]. As reviewed in Chhabra et al. transcripts from the miR-23a~27a~24-2 cluster are altered in different diseases, like colorectal cancer, cardiac hypertrophy or acute myeloid leukemia [23-26]. Actions of the individual miRNAs miR-23a, miR-27a and miR-24-2 have been reported in development and differentiation, as well as in

proliferation and drug resistance [27-29]. A radiation-induced change in expression of the individual cluster members in varying cell types has been reported [30-33]. However, a systematic analysis of the cluster in radiation response is missing.

In this study, we show that ionizing radiation decreases the miR-23a~27a~24-2 cluster expression through two different mechanisms. First on transcriptional level by promoter methylation. Second on post-transcriptional level by AGO complex phosphorylation. We demonstrate that all three mature cluster miRNAs directly affect apoptosis through upregulation of the common target protein XIAP, which is required to prevent apoptosis after radiation exposure.

2. Material and methods

2.1. Cell culture

Human endothelial cells EA.hy926 were grown in DMEM culture medium (Gibco™) supplemented with 1 g/ml D-glucose, 3.7 g/l sodium pyruvate, 10 % FCS and 1xHAT. Human MCF10A breast epithelial cells were cultured in DMEM/F12 (Gibco™) supplemented with 5 % horse serum, 0.5 mg/ml hydrocortisone, 20 ng/ml EGF, 10 µg/ml insulin and 100 ng/ml cholera toxin. Human embryonic kidney cells HEK293FT were grown in DMEM culture medium (Gibco™) supplemented with 4.5 g/ml D-glucose, 3.7 g/l sodium pyruvate, 10 % FCS and 500 µg/ml NEAA. Cells were grown at 37°C in a humidified atmosphere containing 5 % CO_2.

For DNA methyltransferase (DNMT) inhibition EA.hy926 cells were treated with 10 µM of 5-aza-2'deoxycytidine (5-aza-dc, Sigma-Aldrich) in growth medium 3 h prior to irradiation [34]. Control cells were sham-treated with PBS. For RNA polymerase II inhibition EA.hy926 cells were treated with 5 µM of α-amanitin (Sigma-Aldrich) in growth medium as previously

described for endothelial cells [35]. Control cells were sham-treated with H_2O. For stress-response EA.hy926 cells were treated with 5 J UV irradiation, 50 µM cisplatin (Sigma-Aldrich) or 1 µM doxorubicin (Santa Cruz). Control cells were sham-treated. Mycoplasma was ruled out by routine control testing using a luminescence-based detection kit (MykoAlert, Lonza). EA.hy926, MCF10A and HEK293FT cells were authenticated by genetic profiling (Eurofins MWG Operon) with STR matching analysis (DSMZ).

2.2. Irradiation

Irradiation was performed in a Caesium-137 γ-source (HWM-D 2000, Waelischmüller, Germany) operated at a dose rate of 0.46 Gy/min. A dose of 5 Gy was applied at room temperature and control cells were sham-irradiated.

2.3. RNA extraction

For RNA extraction cells ($5x10^5$ cells/treatment) were trypsinized and pelleted at 300 g and 4 °C for 5 min, and washed twice with PBS. Cell pellets were either stored at -20 °C till RNA extraction or immediately processed. Total RNA was extracted with the Maxwell® 16 miRNA Tissue Kit (Promega) and the Maxwell® 16 Instrument (Promega) according to the manufacturer's protocol for cell pellets. The concentration of total RNA was determined using a Nanodrop spectrophometer (PeqLab Biotechnology).

2.4. Quantitative real-time PCR

All qRT-PCR experiments were performed with TaqMan® chemistry according to the manufacturer's instructions. For mRNA and pri-miRNA quantification cDNA was synthesized from 700 ng total RNA using TaqMan® Reverse Transcription Reagents (Applied Biosystems™). For small RNA quantification cDNA was synthesized from 40 ng RNA using

TaqMan®MicroRNA Reverse Transcription Kit (Applied Biosystems™). The qRT-PCR was performed with TaqMan® Universal PCR Master Mix (Applied Biosystems™) and a StepOnePlus Detection System (Applied Biosystems™). Individual biological samples were run in technical duplicates. The relative expression was calculated by normalization to the endogenous control TBP (mRNA and pri-miRNA) and U6 snRNA (miRNAs) and to sham-irradiated control cells using the $2^{-\Delta\Delta CT}$ method.

The following TaqMan™ primer assays were used: pri-miR-23a~27a~24-2 (Hs04270764_pri), hsa-miR-23a-3p (ID: 000399), hsa-miR-23a-5p (ID: 002439), hsa-miR-27a-3p (ID: 000408), hsa-miR-27a-5p (ID: 002445), hsa-miR-24-2 (ID: 002441), U6 snRNA (ID: 001973), (all Thermo Scientific).

For endogenous control TBP (5´-GCCCGAAACGCCGAATAT-3, forward), (5´-CCGTGGTTCGTGGCTCTCT-3, reverse), (5´-ATCCCAAGCGGTTTGCTGCGG-3´, probe), (Eurofins Genomics GmbH) was used.

miRNA hsa-miR-24-1-3p could not be investigated due to the complete homology to the paralog miRNA (miR-24-1-3p, paralog hsa-miR-23b~27b~24-1, see also Fig.1A).

2.5. Promoter Luciferase assay

The promoter region of the hsa-miR~23a~27a~24-2 gene spanning nucleotides -603 to +36 relative to the transcription initiation site was cloned into a promoter-less pGL3-Basic Vector Plasmid (Promega) (see also Fig. 1A) [20]. As positive control a pGL3-Control Vector (Promega), containing a SV40 promoter, was used. For the Luciferase assay 40 ng of Plasmid were transfected in HEK293FT cells using Lipofectamine 2000 transfection reagent (Invitrogen). HEK293FT cells were irradiated 24 h after transfection and promoter activity was measured using the Bright-Glo™ Luciferase Assay System (Promega) according to the manufacturer's protocol and a spectrophotometer plate reader (Tecan). The relative luciferase

activity was determined by normalization of 5 Gy irradiated cells to respective sham-irradiated control cells.

2.6. Immunoblot analysis

EA.hy926 cells were lysed in RIPA buffer (150 mM NaCl, 10 mM Tris-HCl, pH 7.2, 0.1% SDS, 1% Triton X-100, 1% Na-desoxycholate, 5 mM EDTA) supplemented with 1 mM protease inhibitors (sodium orthovanadate and phenylmethanesulfonyl fluoride, Roche) for 20 min on ice. Western blot analysis was performed according to standard procedures using enhanced chemiluminescence detection (Amersham ECL Select Western Blotting Detection Reagent, GE Healthcare Life Science). For detection of the proteins primary antibodies directed against anti-AGO2 (C34C6, #2897, Cell Signaling), pan-AGO (2A8, AGO family, #MABE56, Millipore), phospho-Tyrosine (4G10, #05-321, Upstate), and XIAP (E2, #sc-55551, Santa Cruz Biotechnology) were used. Protein loading was monitored by detection of GAPDH (0411, #sc-47724, Santa Cruz). As secondary antibody goat anti-mouse IgG-HRP (#sc-2005, Santa Cruz Biotechnology) and goat anti-rabbit IgG-HRP (#sc-2004, Santa Cruz Biotechnology) were used to reveal binding of primary antibodies. All western blot analyses were performed in three biological replicates and for quantification of images TotalLab TL 100 software (TotalLab) was used.

2.7. Immunoprecipitation

Immunoprecipitation (IP) was performed with total cell lysates derived from $1x10^7$ EA.hy926 cells. Cells were scrapped, resuspended in 50 µl non-denaturing lysis buffer (150 mM KCl, 25 mM Tris-HCl pH 7.4, 5 mM Na-EDTA pH 8.0, 0.5% Nonidet P-40, 0.5 mM DTT, Protease Inhibitor Cocktail (Sigma-Aldrich)), kept on ice for 5 min and stored overnight at -80 °C [36]. For RNA Immunoprecipitation (RIP) 100 U/ml RNase Inhibitor (Applied Biosystems™) was

added to lysis buffer. The complete lysates were thawed, centrifuged (1200 g, 15 min, 4 °C) and incubated overnight rotating at 4 °C with 5 µg of the antibodies anti-pan-AGO (2A8, AGO family, #MABE56, Millipore), and anti-phospho-Tyrosine (4G10, #05-321, Upstate). IP controls were done with species matched immunoglobulin G (mouse IgG, #12-371, Upstate). 10 % of the complete lysate was kept as input control. 25 µl of Protein G Plus Agarose beads (#IP04, Millipore) were washed twice with 50 µl native lysis buffer. The washed beads were resuspended in 50 µl of the same buffer, added to each lysate-antibody suspension and incubated overnight rotating at 4 °C. Beads were washed three times with lysis buffer, centrifuged (1200 g, 15 min, 4 °C) and further processed for immunoblot analysis or RNA extraction.

2.8. siRNA and miRNA transfection

For RNA transfection $2x10^5$ EA.hy926 cells were seeded into 6 cm culture dishes. 24 h later cells were transfected at a confluency of 50-70% with 100 pmol of a non-specific scrambled control RNA (miRCURY LNA™ negative control A, Exiqon), Pre-miR™ miRNAs (hsa-miR-23a-3p (ID: PM10644), hsa-miR-27a-3p (ID: PM10939), hsa-miR-24-2 (ID: PM12498), Thermo Scientific) or siRNAs (siAGO (ACGGGUCUGUGGUGAUAAATT, Qiagen) and siXIAP (AAGTGCTTTCACTGTGGAGGA, Qiagen)) using Lipofectamine® RNAiMAX Transfection Reagent (Invitrogen™) according to the manufacturer's protocol. Cells were treated with radiation or compound 24 h after transfection.

2.9. *In silico* target identification and network analysis

Ingenuity® Pathway Analysis (IPA®, Ingenuity Systems) was used to identify putative targets of miR-23a, miR-24-2 and miR-27a. Common targets of the miRNAs were analyzed with The microRNA Target Filter (IPA®, Ingenuity Systems), which is based on experimentally

validated interactions from TarBase and miRecords, as well as predicted microRNA-mRNA interactions from TargetScan. Networks of these mRNA genes were then algorithmically generated.

2.10. Dual luciferase assay

Potential binding sites of the individual miR-23a~27a~24-2 cluster miRNAs within the 3'UTR of human XIAP were identified (Supplement A.1) with microRNA.org target prediction [37]. Candidate binding sites sequences were obtained by PCR amplification of reverse transcribed EA.hy926 cell mRNA using the primers indicated in supplementary table A.2 (C1-C8, see also Fig. 4D). The resulting PCR fragments were cloned into the pmirGLO Dual-Luciferase miRNA Target Expression Vector (Promega). The identity and integrity of all constructs was confirmed by DNA sequencing. For luciferase assays 400 pmol of pre-miR-23a, pre-miR-27a, pre-miR-24-2 or the unspecific control oligonucleotides (scr) were transfected along with 40 ng of pmirGLO-3´UTR fusion constructs in EA.hy926 cells using Lipofectamine 2000 transfection reagent (Invitrogen). Luminescence was measured 48 h after transfection using a spectrophotometer plate reader (Tecan). The Firefly luciferase activity was normalized to the Renilla luciferase to compensate for differences in transfection efficiency. The relative luciferase activity was determined as the ratio between the normalized luciferase activities of cells transfected with Pre-miR™ and with unspecific control miRNA.

2.11. Cell cycle analysis

Cell cycle distribution was analyzed 48 h after irradiation by determining the DNA content using propidium iodide (PI) staining and flow cytometry. Cells were harvested and collected by centrifugation at 300 g and 4 °C for 5 min. The cell pellet was washed twice with PBS and either stored at -20 °C till staining or immediately processed. Cell pellets were resuspended in

Cell Cycle Solution (1 g/l NaCitrate, 500 µl/l Triton X-100, 10 mg/l RNase A (bovine pancreas), 50 µg/ml PI) as previously described [38]. Cell cycle distribution was analyzed using a FACScan LSR II (excitation wavelength: 488 nm, emission wavelength: 610 nm; BD Biosciences) and Flowing Software version 2.5.1 (Perttu Terho, Turku Centre for Biotechnology, University of Turku, Finland). Cells with DNA content lower than cells in G1 phase were defined as the subG1 fraction and were considered to be apoptotic.

2.12. Caspase 3/7 activity

To assess apoptosis a Caspase-Glo® 3/7 Assay (Promega) was performed. EA.hy926 cells were seeded into 96-well plates. 24 h later cells were transfected at a confluency of 50-70% with 400 pmol either of control miRNA or specific Pre-miR™ using Lipofectamine® RNAiMAX Transfection Reagent (Invitrogen™) according to the manufacturer's protocol. Irradiation of endothelial EA.hy926 cells was performed 24 h after transfection. Active Caspase 3 and 7 was measured by measuring luminescence using a spectrophotometer plate reader (Tecan) according to the manufacturer's instructions (Caspase-Glo® 3/7 Assay, Promega). Individual biological samples were run in technical triplicates. The relative Caspase activation was calculated by normalization to the sham-irradiated control cells.

2.13. Statistical analysis

Data are presented in figures as mean of biological replicates ± SEM. Significance of n-fold changes was calculated by using the one sample, unpaired, two-tailed student's t-test. Statistical significance was defined as a p-value ≤ 0.05. The p-values are indicated as follows: $*p \leq 0.05$, $**p < 0.01$, $***p < 0.001$.

3. Results

3.1.Stress-induced downregulation of mature miRNAs miR-23a, miR-27a, miR-24-2

The expression of all three mature cluster miRNAs miR-23a, miR-27a, miR-24-2 were decreased after 5 Gy irradiation, being significantly downregulated 24 h after exposure (Fig. 1B). The extent of the decrease varied for each individual miRNA. miR-27a had the greatest change with a fold-change of 0.59 ± 0.07 (Fig. 1B), whereas miR-24-2 was the least decreased with a fold change of 0.79 ± 0.01 at 24 h time point (Fig. 1B). miR-23a exhibited a fold-change of 0.73 ± 0.06 and remained significantly downregulated after 72 h (0.70 ± 0.04), while miR-27a and miR-24-2 had returned to basal levels (Fig. 1B).

The observed changes in the expression of the mature miRNAs were not only present in endothelial EA.hy926 cells after irradiation, but were also identified 48 h after exposure to other stressors, namely UV irradiation, Doxorubicin and Cisplatin (Fig. 1C) or in the non-tumorigenic mammary epithelial cell-line MCF10A 6 h and 8 h after 5 Gy irradiation (Fig. 1D). This underlines the importance of the regulation of the cluster regardless of stress induction or the cell type.

3.2.Radiation-induced methylation leads to reduced pri-miR-23a~27a~24-2 levels

Using quantitative PCR analysis we showed an immediate change in expression for the common primary transcript after a single 5 Gy ɣ-radiation exposure. It was found to be significantly downregulated 2-8 h after irradiation (Fig. 2A). The levels returned to the basal level 24 h after exposure. These results are consistent with the radiation induced downregulation of the individual mature miRNAs (Fig. 1B).

To determine whether reported methylation of the miR-23a~27a~24-2 cluster promoter [21] accounts for the transcriptional change after radiation, methylation was blocked 3 h prior to

radiation using the DNMT inhibitor 5-aza-dc. Equal expression of pri-miR-23a-27a~24-2 in non-irradiated controls (sham-treated and 5-aza-dc treated cells) indicates that the promoter is not significantly affected by methylation under control conditions. After 5 Gy radiation exposure the DNMT inhibition abolished the downregulation of the pri-miR-23a~27a~24-2 transcript at 2 h and 4 h, indicating that radiation-induced changes in transcription of the cluster are at least in part through promoter methylation (Fig. 2B).

In order to confirm if the radiation-induced methylation regulates transcription of the miR-23a~27a~24-2 cluster we conducted a luciferase based reporter assay. The previously published promoter sequence of the cluster was cloned into a promoterless luciferase plasmid [20]. The miR-23a~27a~24-2 promotor increased transcription of the reporter 1.3 fold. Radiation resulted in significantly reduced luciferase activity in comparison to the control plasmids 4 h after 5 Gy irradiation (Fig. 2C).

3.3.Mature miRNAs miR-23a, miR-27a, miR-24-2 are stabilized by AGO

Reduction in expression of the miRNA transcripts may occur post-transcriptionally. Therefore, α-amanitin was used to inhibit polymerase II activity [35]. The primary transcript of the miR-23a~27a~24-2 cluster decreased 4 h after applying α-amanitin and was significantly reduced after 8 h. This is consistent with the time-lag observed after irradiation (Fig. 3A, Fig. 1B). The control transcript TBP decreased after 24 h, indicating the fast turn-over of pri-miR-23a~27a~24-2 (Fig. 3A).

However, the kinetics of the three miRNAs after polymerase II inhibition were very different to that of the primary transcript (Fig. 3B, Fig. 3A). The mature miRNAs were only significantly decreased 48 h after α-amanitin treatment. The much faster rate of reduction seen after

irradiation must therefore include an additional component accelerating degradation (Fig. 3B, Fig. 1B).

Winter and Diederichs demonstrated that miRNAs can be protected from degradation by the Argonaute (AGO) complex [39]. To investigate if radiation influences miR-23a, miR-27a and miR-24-2 stability by affecting AGO binding, we knocked-down AGO2 by siRNA (Fig. 3C) and again inhibited new transcription with α-amanitin. As expected, TBP and pri-miR-23a~27a~24-4 levels were insensitive to the AGO2 knock-down (Suppl. B1), but the mature miRNAs were more rapidly degraded in the absence of the protective AGO2 (Fig. 3D). The miR-23a, miR-27a and miR-24-2 sensitivity to AGO2 knock-down indicates that these miRNAs are stabilized and protected by the AGO complex.

These results were supported by the finding that miR-23a-5p and miR-27a-5p transcripts were indeed insensitive to AGO2 knock-down but were sensitive to α-amanitin, which indicates that these miRNAs are not incorporated into AGO2 (Suppl. B2). Together these findings establish that post-transcriptional stabilization of the mature miRNAs miR-23a-3p, miR-27a-3p, miR-24-2 by AGO may provide a second pathway for rapid reduction in the miRNAs after radiation.

3.4.Radiation destabilizes miR-23a-3p, miR-27a-3p, miR-24-2 by AGO phosphorylation

To obtain information about the incorporation of the cluster miRNAs into the miRISC complex and a possible effect of radiation we performed anti-AGO RNA immunoprecipitation (Suppl. C1). Subsequent qPCR analysis of the pull-down confirmed that miR-23a-3p, miR-27a-3p and miR-24-2 are bound to AGO. Consistent with the AGO2 knock-down results we found that miR-23a-5p and miR-27a-5p are not associated to AGO2 in AGO-pulldown samples (data not shown).

Comparison of AGO-bound miR-23a, miR-27a and miR-24-2 in non-irradiated versus irradiated samples showed a significant reduction of the mature miRNAs 24 h after radiation exposure (Fig. 4A). Control miRNAs that were not regulated by irradiation [31], were included to validate the functionality of the assay. As expected, the abundance of miRNAs miR-93 and miR-222 in AGO pull-down did not change after irradiation (Fig. 4A). The level of miR-16 bound to AGO doubled after irradiation but was not statistically significant ($p = 0.16$) (Fig. 4A). These results demonstrate a selective destabilization of the miRISC complex, which is followed by degradation of the miRNAs miR-23a, miR-27a and miR-24-2.

Shen et al. demonstrated that AGO2 is phosphorylated at position Y393 after hypoxic stress, which is critical for the maturation of certain miRNAs [40]. To study the phosphorylation status of AGO in response to irradiation, we performed anti-phosphotyrosine immunoprecipitation of EA.hy926 lysates. Western blotting of the resulting precipitates with anti-AGO antibody detected 1.8 fold increase in AGO in the phosphorylated protein fraction 24 h after irradiation without a net change in AGO levels after irradiation (Fig. 4B, Suppl. C2, C3). This points to the radiation-induced destabilization of miR-23a, miR-27a and miR-24-2 by AGO phosphorylation as an additional layer of regulation complementing the stress induced transcription of the miR~23a~24-2~27a cluster.

3.5.The miR-23a~27a~24-2 cluster modulates apoptosis after irradiation

Kraemer et al. demonstrated that miRNAs are essential for the survival of endothelial cells following radiation exposure [31]. To investigate the impact of the stress induced downregulated miR-23a~27a~24-2 cluster on cellular survival we analysed apoptosis after overexpression of the individual miRNAs. Overexpression of miR-23a lead to significantly increased SubG1 population (Fig. 5A) and Caspase 3/7 activation (Fig. 5B) in sham-irradiated

and 5 Gy irradiated cells. Interestingly did the overexpression of miR-24-2 also lead to a significant increased apoptosis in irradiated cells, but not in sham irradiated cells (Fig. 5A, B). Whereas miR-27a overexpression just caused significantly increased apoptosis in sham irradiated cells (Fig. 5A, B). Since all three miRNAs displayed an effect on apoptosis and were significantly downregulated after radiation exposure, we hypothesized that the miR-23a~27a~24-2 cluster takes up a synergistic action on cellular survival by regulation of apoptosis. An attempt to simultaneously overexpress the miRNAs failed due to the poor cellular survival after transfection, which underlines the impact of the cluster miRNAs on cell death (data not shown here).

3.6.The miR-23a~27a~24-2 cluster directly interacts with XIAP

In silico target identification using Ingenuity® Pathway analysis identified 6 potential targets that the cluster miRNAs have in common (Fig. 6A). Since the functional characterization showed that overexpression of each miRNA independently increased apoptosis after radiation exposure and that all three miRNAs were downregulated after irradiation, the interaction of the miRNAs with the common predicted target X-linked inhibitor of apoptosis (XIAP) was further tested.

The predicted regulation of XIAP by the miRNAs miR-23a, miR-27a and miR-24-2 was confirmed by western blot analysis 48 h after radiation (Fig. 6B I). Overexpression of each individual cluster miRNA significantly decreased XIAP protein (Fig. 6B II). To establish the nature of XIAP regulation by the cluster miRNAs we performed luciferase reporter assays. Therefore, potential binding sites of the miRNAs to the 3'UTR of the human XIAP were identified with the microRNA.org target prediction tool (Supp. A1) and cloned into a pmiRGlo-reporter plasmid. For miR-23a five potential binding sites were identified (C1, C2, C3, C5, C6)

(Supp. A1). For miR-24-2 one binding site was (C1) found and for miR-27a three binding sites were identified (C2, C4, C6) (Supp. A1). The subsequent analysis confirmed 2 binding sites for miR-23a (C1, C6) and miR-27a (C2, C6) and 1 binding site for miR-24-2 (C1) establishing a direct interaction between five sites in the 3' UTR of human XIAP with the three miRNAs (Fig.6C I-III).

3.7.The miR-23a~27a~24-2 cluster stabilizes XIAP protein levels after irradiation

To further investigate the potential interplay between XIAP and the cluster miRNAs, the kinetics of changes in XIAP protein after irradiation were performed (Fig. 7A I). A significant increase of XIAP protein abundance was observed between 24-72 h (Fig. 7A II) after irradiation. This significant increase agrees well with the observed time dependent decrease in mature miRNA miR-23a, miR-27a and miR-24-2 after irradiation.

Western blot analysis showed that the knock-down of XIAP by siRNA worked efficiently from 24 h after transfection (0 h) to 72 h after irradiation (Fig. 7A I). We hypothesized that the siXIAP mediated knock-down elevates apoptosis in a comparable way to the over-expression of miR-23a, miR-27a and miR-24-2. In support of this hypothesis, FACS analysis revealed a significant increase in apoptosis 48 h after radiation (Fig. 7B). This is also in concordance with the observed significantly increased Caspase 3/7 activity 6 h after radiation (Fig. 7C). These findings provide direct evidence that the miRNAs of the cluster miR-23a~27a~24-2 are stress-induced downregulated to stabilize XIAP protein levels and promote cellular survival.

4. Discussion

In this study, we showed that ionizing radiation decreases the miR-23a~27a~24-2 cluster expression through both, transcription and post-transcriptional processes. The former is by promoter methylation, the latter by AGO complex phosphorylation. We demonstrated that all three mature cluster miRNAs directly affect apoptosis through upregulation of the common target protein XIAP, which is required to prevent apoptosis after radiation exposure.

Previous studies of Kraemer et al. illustrated that the upregulation of specific miRNAs promote endothelial cell survival after irradiation [41]. In addition to this our results evidence that also the downregulation of miRNAs and consequently the stabilization of direct targets contribute to radiation resistance. All three miRNAs displayed a regulatory effect on XIAP expression suggesting a synergistic action on this gene. XIAP is an attractive prognostic marker and therapeutic target in cancer treatment, since it undergoes unique interactions with terminal effector caspases and can act as block for apoptosis [42-45]. It has been shown to be often deregulated in different cancers, which can also affect cancer treatment [46-48]. Radiation induced upregulation of XIAP in radiation resistant human carcinoma cells increases resistance to radiation induced cell death [49, 50]. New insights on XIAP regulation and overcoming drug resistance suggest miRNAs targeting XIAP as attractive application in cancer treatment [51, 52]. In compliance it has been shown that miR-23a, miR-27a and miR-24 also synergistically regulate the JAK1/Stat3 signalling in human erythroid leukaemia and thereby affect apoptosis and proliferation [53]. Consequently, the miR-23a~27a~24-2 cluster and its regulation presents an attractive target to modify apoptosis for individual cancer therapy.

Several reports show transcriptional regulation through miRNA promoter methylation [54-57]. Evidence for a link between transcriptional repression and methylation of the cluster promoter comes from the study of Wang and Zhang et al. [21]. These authors showed that demethylated SP1 sites in GC-rich regions of the cluster promoter result in over-expression of hsa-miR-23a~27a~24-2 in laryngeal cancer cells. Our study indicates a radiation-induced methylation

of the cluster promoter to suppress hsa-miR-23a~27a~24-2 cluster miRNA abundance. This establishes that the methylation status of the hsa-miR-23a~27a~24-2 promoter is important for its transcription and can be rapidly changed by stress induction. However, after transcriptional blockage the levels of the mature miRNAs were decreased considerably slower than after irradiation.

To explain this time lapse our transcriptional blockage and AGO-knock-down results suggest an additional post-transcriptional destabilization. Correspondingly, Winter and Diederichs provide evidence that AGO proteins stabilize mature miRNAs [39]. Indeed, immunoprecipitation with consecutive miRNA expression analysis revealed that radiation reduces selectively cluster miRNA binding. Rüdel et al. demonstrated that phosphorylation of AGO proteins affects miRNA binding, which can be affirmed by our findings [58]. A stress induced altered maturation of a subset of miRNAs by AGO phosphorylation might be mediated by EGFR signalling as shown after hypoxia [40]. Since the terminal loop of a miRNA is crucial to Drosha cleavage [59, 60], an association between genetic variants of pre-miR-27a loop-structure and familial breast cancer risk has been identified [61]. Therefore an additional contribution of other turn-over mechanisms or epigenetic changes upon radiation may be possible [62-64].

In summary, we report two different stress-induced regulatory mechanisms, which influence the cluster and are essential to assure a time-dependent signalling cascade, allowing cellular survival after stress. Hence, it is not only important to elucidate the regulation and function of the hsa-miR-23a~27a~24-2 cluster, but also to investigate the therapeutic potential of the cluster on cellular survival in cancer treatment.

Acknowledgement

The authors thank Rosemarie Kell for her excellent technical assistance.

Funding

This research did not receive any specific grant from funding agencies in the public, commercial, or not-for-profit sectors.

References

[1] W. Filipowicz, S.N. Bhattacharyya, N. Sonenberg, Mechanisms of post-transcriptional regulation by microRNAs: are the answers in sight?, Nat Rev Genet, 9 (2008) 102-114.
[2] M.R. Fabian, N. Sonenberg, The mechanics of miRNA-mediated gene silencing: a look under the hood of miRISC, Nat Struct Mol Biol, 19 (2012).
[3] K.P. Porkka, M.J. Pfeiffer, K.K. Waltering, R.L. Vessella, T.L.J. Tammela, T. Visakorpi, MicroRNA Expression Profiling in Prostate Cancer, Cancer Research, 67 (2007) 6130-6135.
[4] S. Volinia, G.A. Calin, C.-G. Liu, S. Ambs, A. Cimmino, F. Petrocca, R. Visone, M. Iorio, C. Roldo, M. Ferracin, R.L. Prueitt, N. Yanaihara, G. Lanza, A. Scarpa, A. Vecchione, M. Negrini, C.C. Harris, C.M. Croce, A microRNA expression signature of human solid tumors defines cancer gene targets, Proceedings of the National Academy of Sciences of the United States of America, 103 (2006) 2257-2261.
[5] J. Hausser, M. Zavolan, Identification and consequences of miRNA-target interactions [mdash] beyond repression of gene expression, Nat Rev Genet, 15 (2014) 599-612.
[6] M. Davari, Z.-S. Soheili, S. Samiei, Z. Sharifi, E.R. Pirmardan, Overexpression of miR-183/-96/-182 triggers neuronal cell fate in Human Retinal Pigment Epithelial (hRPE) cells in culture, Biochemical and Biophysical Research Communications, 483 (2017) 745-751.
[7] J. Yu, F. Wang, G.H. Yang, F.L. Wang, Y.N. Ma, Z.W. Du, J.W. Zhang, Human microRNA clusters: genomic organization and expression profile in leukemia cell lines, Biochem Biophys Res Commun, 349 (2006).
[8] A. Kraemer, N. Anastasov, M. Angermeier, K. Winkler, M.J. Atkinson, S. Moertl, MicroRNA-mediated processes are essential for the cellular radiation response, Radiation research, 176 (2011) 575-586.
[9] O.C. Maes, J. An, H. Sarojini, H. Wu, E. Wang, Changes in MicroRNA expression patterns in human fibroblasts after low-LET radiation, Journal of cellular biochemistry, 105 (2008) 824-834.
[10] M. Wagner-Ecker, C. Schwager, U. Wirkner, A. Abdollahi, P.E. Huber, MicroRNA expression after ionizing radiation in human endothelial cells, Radiation oncology, 5 (2010) 25.
[11] P. Ahmad, J. Sana, M. Slavik, P. Slampa, P. Smilek, O. Slaby, MicroRNAs Involvement in Radioresistance of Head and Neck Cancer, Disease Markers, 2017 (2017) 8245345.

[12] X.C. Wang, L.Q. Du, L.L. Tian, H.L. Wu, X.Y. Jiang, H. Zhang, D.G. Li, Y.Y. Wang, H.Y. Wu, Y. She, Q.F. Liu, F.Y. Fan, A.M. Meng, Expression and function of miRNA in postoperative radiotherapy sensitive and resistant patients of non-small cell lung cancer, Lung Cancer, 72 (2011) 92-99.

[13] L. Zhao, X. Lu, Y. Cao, MicroRNA and Signal Transduction Pathways in Tumor Radiation Response, Cellular signalling, 25 (2013) 1625-1634.

[14] I. Summerer, K. Unger, H. Braselmann, L. Schuettrumpf, C. Maihoefer, P. Baumeister, T. Kirchner, M. Niyazi, E. Sage, H.M. Specht, G. Multhoff, S. Moertl, C. Belka, H. Zitzelsberger, Circulating microRNAs as prognostic therapy biomarkers in head and neck cancer patients, British Journal of Cancer, 113 (2015) 76-82.

[15] J.S. Dickey, F.J. Zemp, O.A. Martin, O. Kovalchuk, The role of miRNA in the direct and indirect effects of ionizing radiation, Radiation and Environmental Biophysics, 50 (2011) 491.

[16] M. Winther, S. Knudsen, J. Dahlgaard, T. Jensen, A. Hansen, P.B. Jensen, T. Tramm, J. Alsner, M. Nordsmark, Clinical Impact of a Novel MicroRNA Chemo-Sensitivity Predictor in Gastrooesophageal Cancer, PLOS ONE, 11 (2016) e0148070.

[17] S. Moertl, L. Mutschelknaus, T. Heider, M.J. Atkinson, MicroRNAs as novel elements in personalized radiotherapy, Translational Cancer Research, (2016) S1262-S1269.

[18] M. He, W. Zhou, C. Li, M. Guo, MicroRNAs, DNA Damage Response, and Cancer Treatment, International Journal of Molecular Sciences, 17 (2016) 2087.

[19] C. Zhang, G. Peng, Non-coding RNAs: An emerging player in DNA damage response, Mutation Research/Reviews in Mutation Research, 763 (2015) 202-211.

[20] Y. Lee, M. Kim, J. Han, K.H. Yeom, S. Lee, S.H. Baek, V.N. Kim, MicroRNA genes are transcribed by RNA polymerase II, EMBO J, 23 (2004).

[21] Y. Wang, Z.-X. Zhang, S. Chen, G.-B. Qiu, Z.-M. Xu, W.-N. Fu, Methylation Status of SP1 Sites within miR-23a-27a-24-2 Promoter Region Influences Laryngeal Cancer Cell Proliferation and Apoptosis, BioMed Research International, 2016 (2016) 2061248.

[22] M. Lagos-Quintana, R. Rauhut, W. Lendeckel, T. Tuschl, Identification of Novel Genes Coding for Small Expressed RNAs, Science, 294 (2001) 853.

[23] Y. Xi, R. Shalgi, O. Fodstad, Y. Pilpel, J. Ju, Differentially Regulated Micro-RNAs and Actively Translated Messenger RNA Transcripts by Tumor Suppressor p53 in Colon Cancer, Clinical Cancer Research, 12 (2006) 2014.

[24] R. Chhabra, R. Dubey, N. Saini, Cooperative and individualistic functions of the microRNAs in the miR-23a~27a~24-2 cluster and its implication in human diseases, Molecular Cancer, 9 (2010) 232.
[25] Z. Lin, I. Murtaza, K. Wang, J. Jiao, J. Gao, P.-F. Li, miR-23a functions downstream of NFATc3 to regulate cardiac hypertrophy, Proceedings of the National Academy of Sciences of the United States of America, 106 (2009) 12103-12108.
[26] S. Mi, J. Lu, M. Sun, Z. Li, H. Zhang, M.B. Neilly, Y. Wang, Z. Qian, J. Jin, Y. Zhang, S.K. Bohlander, M.M. Le Beau, R.A. Larson, T.R. Golub, J.D. Rowley, J. Chen, MicroRNA expression signatures accurately discriminate acute lymphoblastic leukemia from acute myeloid leukemia, Proceedings of the National Academy of Sciences of the United States of America, 104 (2007) 19971-19976.
[27] V. Moresi, N. Marroncelli, D. Coletti, S. Adamo, Regulation of skeletal muscle development and homeostasis by gene imprinting, histone acetylation and microRNA, Biochimica et Biophysica Acta (BBA) - Gene Regulatory Mechanisms, 1849 (2015) 309-316.
[28] Z. Wang, W. Wei, F.H. Sarkar, miR-23a, a critical regulator of "migR"ation and metastasis in colorectal cancer, Cancer Discovery, 2 (2012) 489-491.
[29] M.Q. Hassan, J.A.R. Gordon, M.M. Beloti, C.M. Croce, A.J.v. Wijnen, J.L. Stein, G.S. Stein, J.B. Lian, A network connecting Runx2, SATB2, and the miR-23a~27a~24-2 cluster regulates the osteoblast differentiation program, Proceedings of the National Academy of Sciences, 107 (2010) 19879-19884.
[30] N. McDermott, A. Meunier, S. Wong, V. Buchete, L. Marignol, Profiling of a panel of radioresistant prostate cancer cells identifies deregulation of key miRNAs, Clinical and Translational Radiation Oncology, 2 (2017) 63-68.
[31] A. Kraemer, N. Anastasov, M. Angermeier, K. Winkler, M.J. Atkinson, S. Moertl, MicroRNA-Mediated Processes are Essential for the Cellular Radiation Response, Radiation Research, 176 (2011) 575-586.
[32] C. Metheetrairut, F.J. Slack, MicroRNAs in the ionizing radiation response and in radiotherapy, Curr Opin Genet Dev, 23 (2013).
[33] S.S. Acharya, W. Fendler, J. Watson, A. Hamilton, Y. Pan, E. Gaudiano, P. Moskwa, P. Bhanja, S. Saha, C. Guha, K. Parmar, D. Chowdhury, Serum microRNAs are early indicators of survival after radiation-induced hematopoietic injury, Science Translational Medicine, 7 (2015) 287ra269-287ra269.

[34] S.S. Palii, B.O. Van Emburgh, U.T. Sankpal, K.D. Brown, K.D. Robertson, DNA Methylation Inhibitor 5-Aza-2′-Deoxycytidine Induces Reversible Genome-Wide DNA Damage That Is Distinctly Influenced by DNA Methyltransferases 1 and 3B, Molecular and Cellular Biology, 28 (2008) 752-771.

[35] E. Rydkina, A. Sahni, R.B. Baggs, D.J. Silverman, S.K. Sahni, Infection of Human Endothelial Cells with Spotted Fever Group Rickettsiae Stimulates Cyclooxygenase 2 Expression and Release of Vasoactive Prostaglandins, Infection and Immunity, 74 (2006) 5067-5074.

[36] D.G. Hendrickson, D.J. Hogan, H.L. McCullough, J.W. Myers, D. Herschlag, J.E. Ferrell, P.O. Brown, Concordant Regulation of Translation and mRNA Abundance for Hundreds of Targets of a Human microRNA, PLoS Biology, 7 (2009) e1000238.

[37] D. Betel, M. Wilson, A. Gabow, D.S. Marks, C. Sander, The microRNA.org resource: targets and expression, Nucleic Acids Research, 36 (2008) D149-D153.

[38] C. Riccardi, I. Nicoletti, Analysis of apoptosis by propidium iodide staining and flow cytometry, Nat. Protocols, 1 (2006) 1458-1461.

[39] J. Winter, S. Diederichs, Argonaute proteins regulate microRNA stability: Increased microRNA abundance by Argonaute proteins is due to microRNA stabilization, RNA Biology, 8 (2011) 1149-1157.

[40] J. Shen, W. Xia, Y.B. Khotskaya, L. Huo, K. Nakanishi, S.-O. Lim, Y. Du, Y. Wang, W.-C. Chang, C.-H. Chen, J.L. Hsu, Y. Wu, Y.C. Lam, B.P. James, X. Liu, C.-G. Liu, D.J. Patel, M.-C. Hung, EGFR modulates microRNA maturation in response to hypoxia through phosphorylation of AGO2, Nature, 497 (2013) 383-387.

[41] A. Kraemer, Z. Barjaktarovic, H. Sarioglu, K. Winkler, F. Eckardt-Schupp, S. Tapio, M.J. Atkinson, S. Moertl, Cell Survival Following Radiation Exposure Requires miR-525-3p Mediated Suppression of ARRB1 and TXN1, PLoS ONE, 8 (2013) e77484.

[42] L. Flanagan, J. Kehoe, J. Fay, O. Bacon, A.U. Lindner, E.W. Kay, J. Deasy, D.A. McNamara, J.H.M. Prehn, High levels of X-linked Inhibitor-of-Apoptosis Protein (XIAP) are indicative of radio chemotherapy resistance in rectal cancer, Radiation Oncology, 10 (2015) 131.

[43] M. Holcik, H. Gibson, R.G. Korneluk, XIAP: Apoptotic brake and promising therapeutic target, Apoptosis, 6 (2001) 253-261.

[44] P. Obexer, M.J. Ausserlechner, X-Linked Inhibitor of Apoptosis Protein – A Critical Death Resistance Regulator and Therapeutic Target for Personalized Cancer Therapy, Frontiers in Oncology, 4 (2014).
[45] S. Hehlgans, C. Petraki, S. Reichert, N. Cordes, C. Rödel, F. Rödel, Double targeting of Survivin and XIAP radiosensitizes 3D grown human colorectal tumor cells and decreases migration, Radiotherapy and Oncology, 108 (2013) 32-39.
[46] E. Strekalova, D. Malin, H. Rajanala, V.L. Cryns, Metformin sensitizes triple-negative breast cancer to proapoptotic TRAIL receptor agonists by suppressing XIAP expression, Breast Cancer Research and Treatment, (2017) 1-13.
[47] D.-G. Wang, Y.-B. Sun, F. Ye, W. Li, P. Kharbuja, L. Gao, D.Y. Zhang, J. Suo, Anti-tumor activity of the X-linked inhibitor of apoptosis (XIAP) inhibitor embelin in gastric cancer cells, Molecular and Cellular Biochemistry, 386 (2014) 143-152.
[48] T. Shibata, C. Mahotka, N. Wethkamp, S. Heikaus, H.E. Gabbert, U. Ramp, Disturbed Expression of the Apoptosis Regulators XIAP, XAF1, and Smac/DIABLO in Gastric Adenocarcinomas, Diagnostic Molecular Pathology, 16 (2007) 1-8.
[49] D. Moussata, S. Amara, B. Siddeek, M. Decaussin, S. Hehlgans, R. Paul-Bellon, F. Mornex, J.-P. Gerard, P. Romestaing, F. Rödel, B. Flourie, M. Benahmed, C. Mauduit, XIAP as a Radioresistance Factor and Prognostic Marker for Radiotherapy in Human Rectal Adenocarcinoma, The American Journal of Pathology, 181 1271-1278.
[50] C. Cao, Y. Mu, D.E. Hallahan, B. Lu, XIAP and survivin as therapeutic targets for radiation sensitization in preclinical models of lung cancer, Oncogene, 23 (2004) 7047-7052.
[51] S. Zhou, Q. Huang, S. Zheng, K. Lin, J. You, X. Zhang, miR-27a regulates the sensitivity of breast cancer cells to cisplatin treatment via BAK-SMAC/DIABLO-XIAP axis, Tumor Biology, 37 (2016) 6837-6845.
[52] X. Li, W. Chen, W. Zeng, C. Wan, S. Duan, S. Jiang, microRNA-137 promotes apoptosis in ovarian cancer cells via the regulation of XIAP, Br J Cancer, 116 (2017) 66-76.
[53] R. Su, L. Dong, D. Zou, H. Zhao, Y. Ren, F. Li, P. Yi, L. Li, Y. Zhu, Y. Ma, J. Wang, F. Wang, J. Yu, microRNA-23a, -27a and -24 synergistically regulate JAK1/Stat3 cascade and serve as novel therapeutic targets in human acute erythroid leukemia, Oncogene, 35 (2016) 6001-6014.
[54] H. Siemens, J. Neumann, R. Jackstadt, U. Mansmann, D. Horst, T. Kirchner, H. Hermeking, Detection of miR-34a Promoter Methylation in Combination with Elevated

Expression of c-Met and β-Catenin Predicts Distant Metastasis of Colon Cancer, Clinical Cancer Research, 19 (2013) 710-720.
[55] Z. Li, H. Lei, M. Luo, Y. Wang, L. Dong, Y. Ma, C. Liu, W. Song, F. Wang, J. Zhang, J. Shen, J. Yu, DNA methylation downregulated mir-10b acts as a tumor suppressor in gastric cancer, Gastric Cancer, 18 (2015) 43-54.
[56] S. Zhang, J. Hao, F. Xie, X. Hu, C. Liu, J. Tong, J. Zhou, J. Wu, C. Shao, Downregulation of miR-132 by promoter methylation contributes to pancreatic cancer development, Carcinogenesis, 32 (2011) 1183-1189.
[57] F. Parodi, R. Carosio, M. Ragusa, C. Di Pietro, M. Maugeri, D. Barbagallo, F. Sallustio, G. Allemanni, M.P. Pistillo, I. Casciano, A. Forlani, F.P. Schena, M. Purrello, M. Romani, B. Banelli, Epigenetic dysregulation in neuroblastoma: A tale of miRNAs and DNA methylation, Biochimica et Biophysica Acta (BBA) - Gene Regulatory Mechanisms, 1859 (2016) 1502-1514.
[58] S. Rüdel, Y. Wang, R. Lenobel, R. Körner, H.-H. Hsiao, H. Urlaub, D. Patel, G. Meister, Phosphorylation of human Argonaute proteins affects small RNA binding, Nucleic Acids Research, 39 (2011) 2330-2343.
[59] Y. Zeng, R. Yi, B.R. Cullen, Recognition and cleavage of primary microRNA precursors by the nuclear processing enzyme Drosha, The EMBO Journal, 24 (2005) 138-148.
[60] J. Krol, I. Loedige, W. Filipowicz, The widespread regulation of microRNA biogenesis, function and decay, Nat Rev Genet, 11 (2010) 597-610.
[61] R. Yang, B. Schlehe, K. Hemminki, C. Sutter, P. Bugert, B. Wappenschmidt, J. Volkmann, R. Varon, B.H.F. Weber, D. Niederacher, N. Arnold, A. Meindl, C.R. Bartram, R.K. Schmutzler, B. Burwinkel, A genetic variant in the pre-miR-27a oncogene is associated with a reduced familial breast cancer risk, Breast Cancer Research and Treatment, 121 (2010) 693-702.
[62] B.D. Adams, K.P. Claffey, B.A. White, Argonaute-2 Expression Is Regulated by Epidermal Growth Factor Receptor and Mitogen-Activated Protein Kinase Signaling and Correlates with a Transformed Phenotype in Breast Cancer Cells, Endocrinology, 150 (2009) 14-23.
[63] V. Libri, P. Miesen, R.P. van Rij, A.H. Buck, Regulation of microRNA biogenesis and turnover by animals and their viruses, Cellular and Molecular Life Sciences, 70 (2013) 3525-3544.

[64] J. Krell, J. Stebbing, C. Carissimi, A.F. Dabrowska, A. de Giorgio, A.E. Frampton, V. Harding, V. Fulci, G. Macino, T. Colombo, L. Castellano, TP53 regulates miRNA association with AGO2 to remodel the miRNA–mRNA interaction network, Genome Research, 26 (2016) 331-341.

Figure 1: Stress-induced downregulation of mature miRNAs miR-23a, miR-27a and miR-24-2

A) I) The structure of the 2159 nt hsa-miR-23a~27a~24-2 cluster (Chr19: 13836587-13836359 [-]). The promoter region is spanning from -603 to +36 relative to the transcription initiation site (+1).
II) The structure of the paralog hsa-miR-23b~27b~24-1 (Chr9: 95085208-95086088 [+]). The paralog cluster is located within the C9orf3 gene.

B) Relative expression of the mature miRNAs of the miR-23a~27a~24-2 cluster at 0.5-72 h in endothelial EA.hy926 cells after exposure to 5 Gy of irradiation. Changes in expression were calculated by normalization to the housekeeping TBP and sham-irradiated control cells (set as 1). Data represent means ± SEM. n = 3, $*p \leq 0.05$, $**p \leq 0.01$.

C) Relative expression of the mature miRNAs of the miR-23a~27a~24-2 cluster at 48 h after exposure to 5 J UV radiation, 50 µM cisplatin, 1 µM doxorubicin. Changes in expression were calculated by normalization to the housekeeping snoRNA U6 and sham-treated control cells (set as 1). Data represent means ± SEM, n = 3, $*p \leq 0.05$, $**p \leq 0.01$.

D) Relative expression of the mature miRNAs of the miR-23a~27a~24-2 cluster at 4-24 h in mammary epithelial MCF10A cells after exposure to 5 Gy of irradiation. Changes in expression were calculated by normalization to the housekeeping snoRNA U6 and sham-irradiated control cells (set as 1). Data represent means ± SEM, n = 3, $*p \leq 0.05$, $**p \leq 0.01$.

Figure 2: Radiation-induced methylation leads to reduced pri-23a~27a~24-2

A) Relative expression of the primary transcript of the miR-23a~27a~24-2 cluster at 0.5-72 h after exposure to 5 Gy of irradiation. Changes in expression were calculated by normalization to the housekeeping TBP and sham-irradiated control cells (set as 1). Data represent means ± SEM, n = 3, $*p \leq 0.05$, $**p \leq 0.01$.

B) EA.hy926 cells were treated with 10 µM of 5-aza-2'deoxycytidine (5-aza-dc) for DNMT inhibition 3 h prior to 5 Gy irradiation. Control cells were sham-treated with PBS. Changes in expression were calculated by normalization to the housekeeping TBP and sham-irradiated control cells (set as 1). Data represent means ± SEM, n = 3, $*p \leq 0.05$, $**p \leq 0.01$.

C) HEK293FT cells were transfected with different luciferase pGl3 vector plasmids, either lacking a promoter (pGL3-basic), or with inserted hsa-miR-23a~27a~24-2 promoter (pGL3-promoter), or a plasmid containing a SV40-promoter (pGL3-control). Luciferase activity was analyzed 4 h after 5 Gy irradiation and changes were calculated by normalization to sham-irradiated control cells. Changes in Data represent means ± SEM, n = 3, $*p \leq 0.05$, $**p \leq 0.01$.

Figure 3: miR-23a, miR-27a and miR-24-2 are stabilized by AGO complex

A/B) EA.hy926 cells were treated with 5 μM of α-amanitin for transcriptional inhibition. Relative Expression was measured 4-48 h after treatment. Changes in expression were calculated by normalization to sham-treated control cells. Data represent means ± SEM, n = 3, $*p \leq 0.05$, $**p \leq 0.01$, $***p \leq 0.001$.
C) Representative western blot of EA.hy926 cells transfected with siRNA against AGO2 24 h to 72h after transfection.
D) EA.hy926 cells were transfected with siRNA against AGO2. 24 h after transfection cells were treated with 5 μM of α-amanitin for transcriptional inhibition. Relative expression was measured 24 h after treatment. Changes in expression were calculated by normalization to respectively-treated control cells. Data represent means ± SEM, n = 3, $*p \leq 0.05$, $**p \leq 0.01$, $***p \leq 0.001$.

Figure 4: radiation induced destabilization of AGO complex

A) Relative abundance of miRNAs bound to AGO in immunoprecipitates measured 24 h after 5 Gy irradiation with Realtime PCR. Pull-down was either directed against pan-AGO or against unspecific IgG control Changes in expression were calculated by normalization to the respective unspecific IgG control and sham-irradiated control immunoprecipitates. Data represent means with ± SEM, n = 3, $*p \leq 0.05$, $**p \leq 0.01$.
B) Relative abundance of AGO phosphorylated in tyrosine measured with Western Blot in immunoprecipitates 24 h after 5 Gy irradiation. Pull-down was either directed against pTyr or against unspecific IgG control. Changes in pan-AGO protein level were calculated by normalization to the respective unspecific IgG control and sham-irradiated control immunoprecipitates. Data represent means with ± SEM, n = 3, $*p \leq 0.05$, $**p \leq 0.01$.

Figure 5: Effect of miR-23a, miR-27a and miR-24-2 on apoptosis

A) FACS analysis of apoptotic EA.hy926 cells that were transfected with pre-miRNAs 24 h prior to 5 Gy or sham-irradiation. Changes in SubG1 population 48 h after radiation were calculated by normalization to the sham-irradiated unspecific RNA control. Data represent means with ± SEM, n = 3, $*p \leq 0.05$, $**p \leq 0.01$.
B) EA.hy926 cells were transfected with pre-miRNAs 24 h prior to 5 Gy or sham-irradiation. Cells were analysed with Caspase-Glo® 3/7 Assay 6 h after 5 Gy or sham-irradiation. Changes were calculated by normalization to the sham-irradiated unspecific RNA control. Data represent means with ± SEM, n = 3, $*p \leq 0.05$, $**p \leq 0.01$.

Figure 6: miR-23a, miR-27a and miR-24-2 directly interact with XIAP

A) *In silico* target analysis of common targets of the miRNA-cluster hsa-miR-23a~27a~24-2 with Ingenuity pathway analysis (IPA®).
B) EA.hy926 cells were transfected with unspecific control RNAs or pre-miRNAs 24 h prior to 5 Gy or sham-irradiation. I) Representative XIAP western blot 48 h after irradiation. II) Changes in XIAP protein abundance 48 h after irradiation were

calculated by normalisation to GAPDH and the sham-irradiated unspecific RNA control. Significance was determined by comparison of individual overexpressed miRNAs with respectively irradiated control. Data represent means with ± SEM, n = 3, $*p \leq 0.05$, $**p \leq 0.01$.

C) Subsequent direct target confirmation with Dual-Luciferase® Reporter Assay 48 h after transfection. I) 5 potential binding sites for miR-23a (C1, C2, C3, C5, C6). II) 1 potential binding site for miR-24-2 (C1). III) 3 potential binding sites for miR-27a (C2, C4, C6). Changes were calculated by normalization to pmiRGlo unspecific RNA control. Data represent means with ± SEM, n = 3, $*p \leq 0.05$, $**p \leq 0.01$.

Figure 7: miR-23a~27a~24-2 cluster stabilizes XIAP after irradiation

A) EA.hy926 cells were transfected with unspecific control RNA or siXIAP 24 h prior to 5 Gy or sham-irradiation. I) Representative XIAP western blot of EA.hy926 cells 0-72 h after 5 Gy irradiation. II) Changes in XIAP protein abundance 6-72 h after irradiation were calculated by normalisation to GAPDH and the sham-irradiated unspecific RNA control. Data represent means with ± SEM, n = 3, $*p \leq 0.05$, $**p \leq 0.01$.

B) FACS analysis of apoptotic EA.hy926 cells that were transfected with siRNA against XIAP 24 h prior to 5 Gy or sham-irradiation. Changes in SubG1 population 48 h after irradiation were calculated by normalization to the sham-irradiated unspecific RNA control. Significance was determined by comparison of individual overexpressed miRNAs with respectively irradiated control. Data represent means with ± SEM, n = 3, $*p \leq 0.05$, $**p \leq 0.01$.

C) EA.hy926 cells were transfected with siRNA against XIAP 24 h prior to 5 Gy or sham-irradiation. Cells were analysed with Caspase-Glo® 3/7 Assay 6 h after 5 Gy or sham-irradiation. Changes were calculated by normalization to the sham-irradiated unspecific RNA control. Significance was determined by comparison of individual overexpressed miRNAs with respectively irradiated control. Data represent means with ± SEM, n = 3, $*p \leq 0.05$, $**p \leq 0.01$.

Figure 1

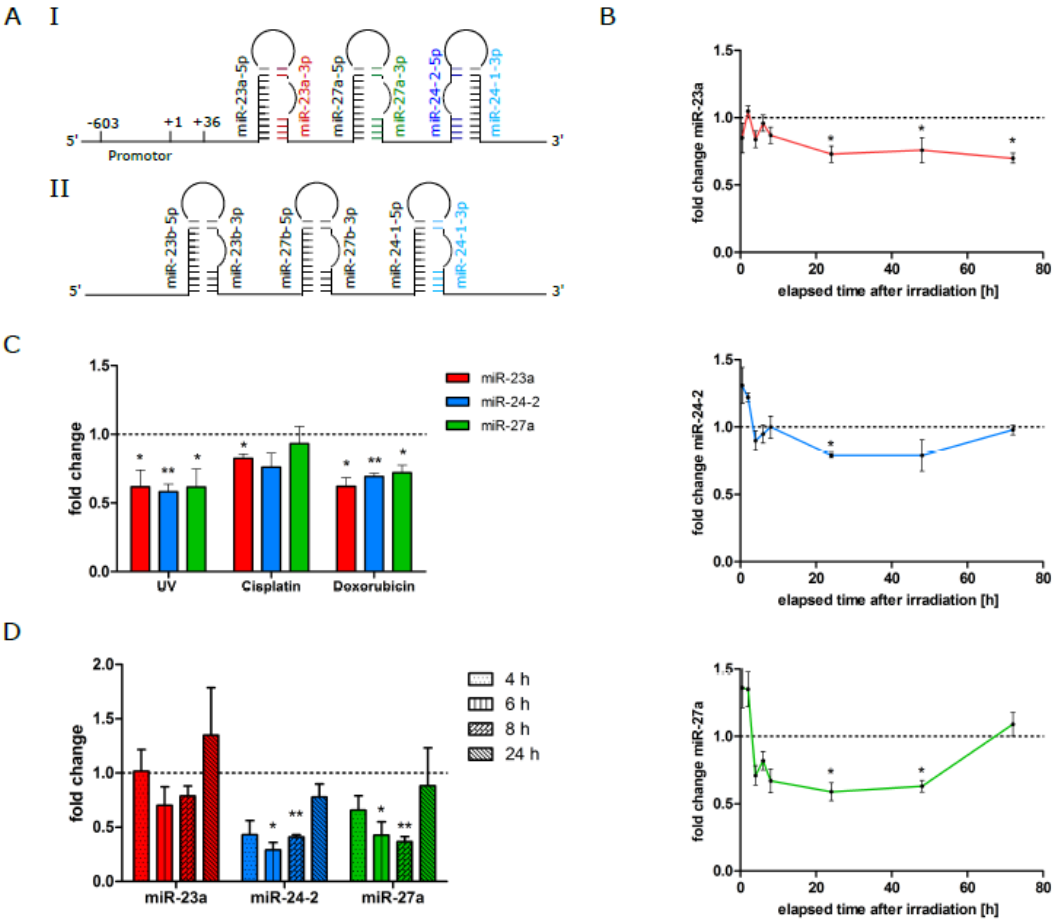

Figure 2

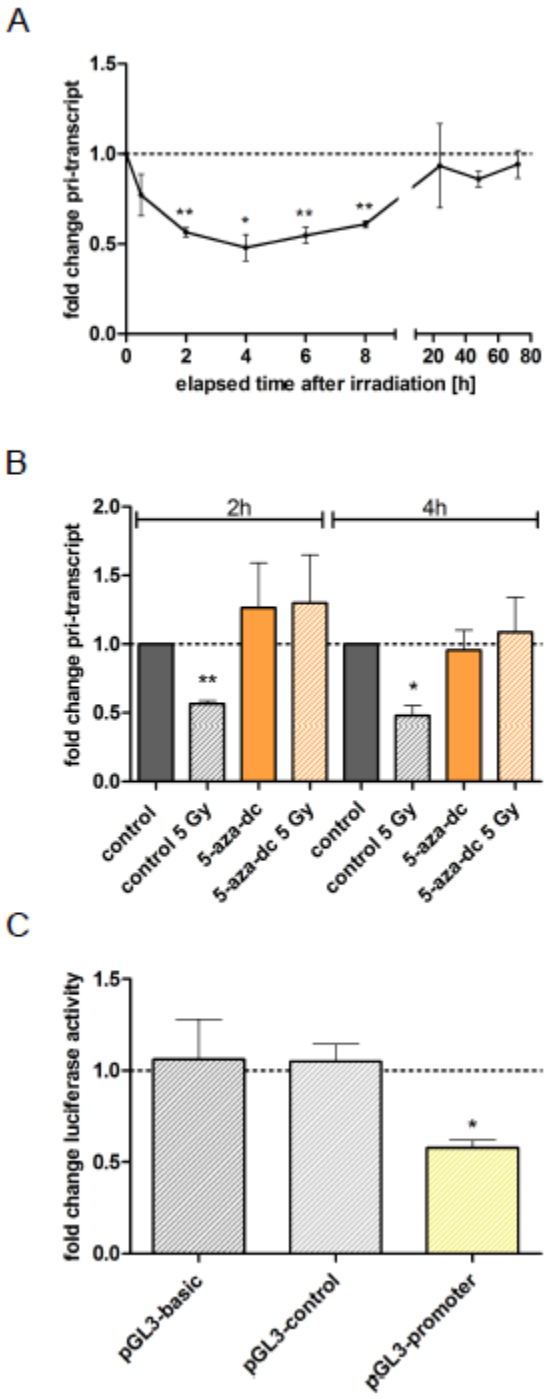

Figure 3

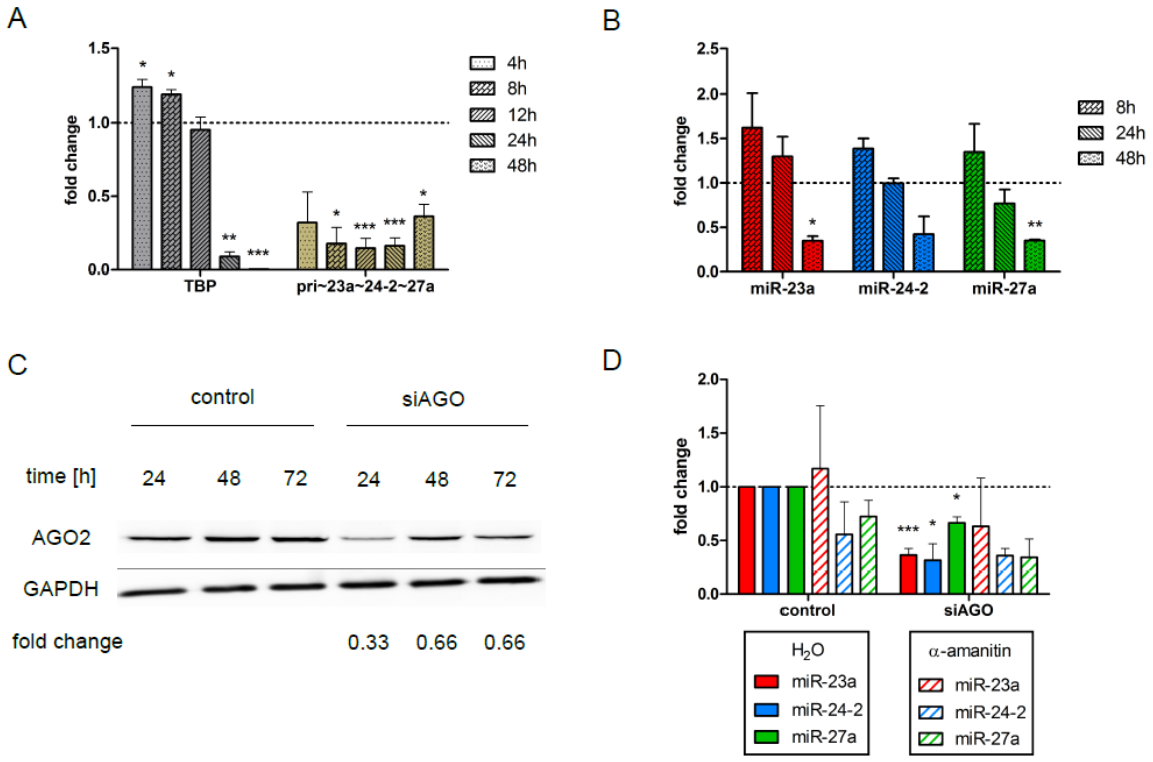

Figure 4

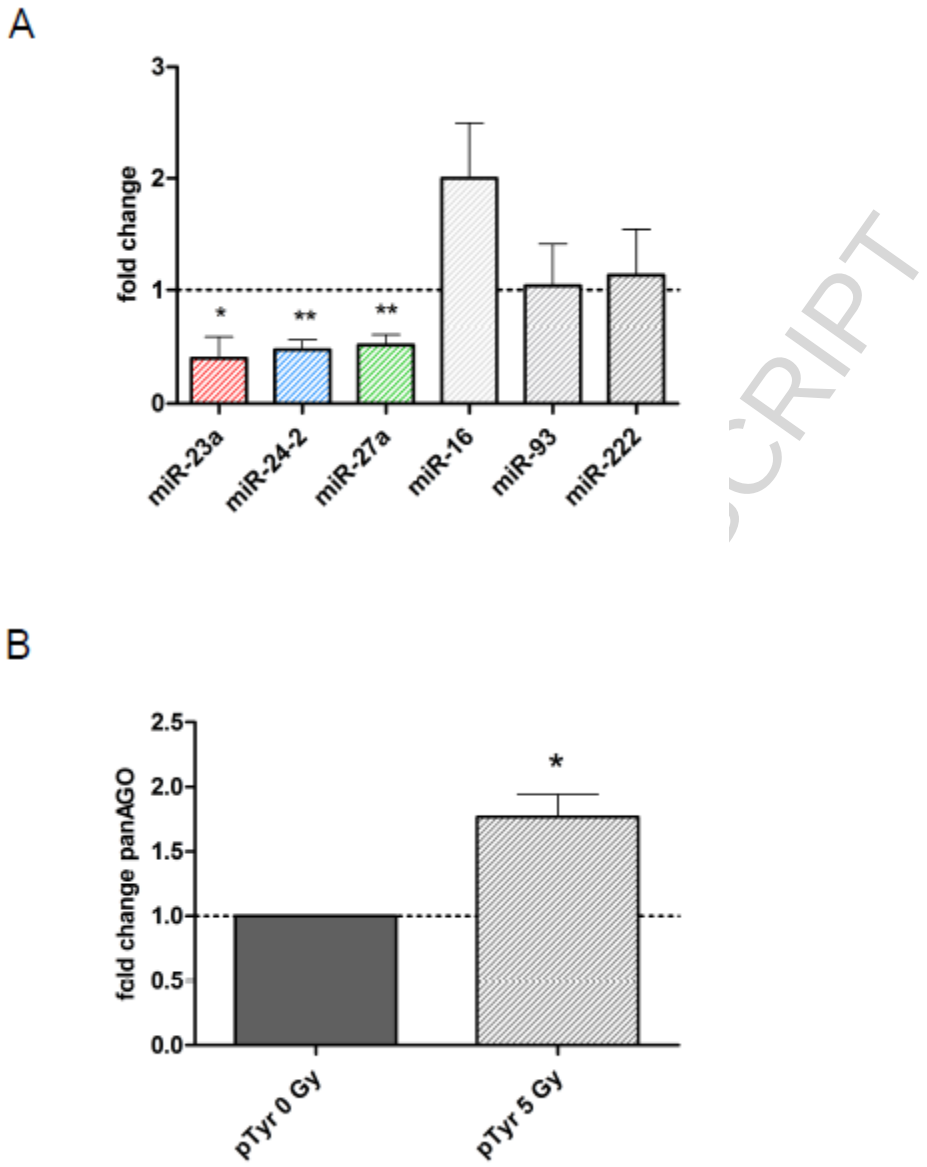

Figure 5

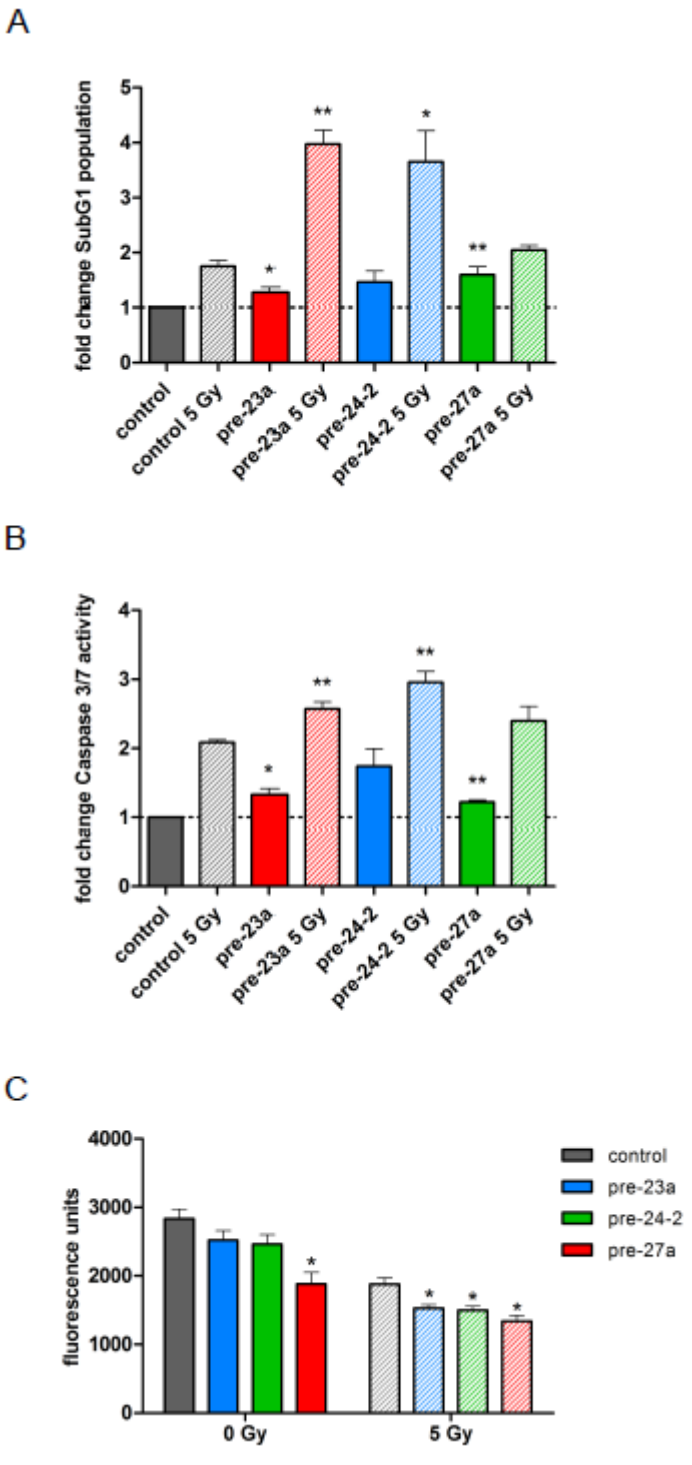

Figure 6

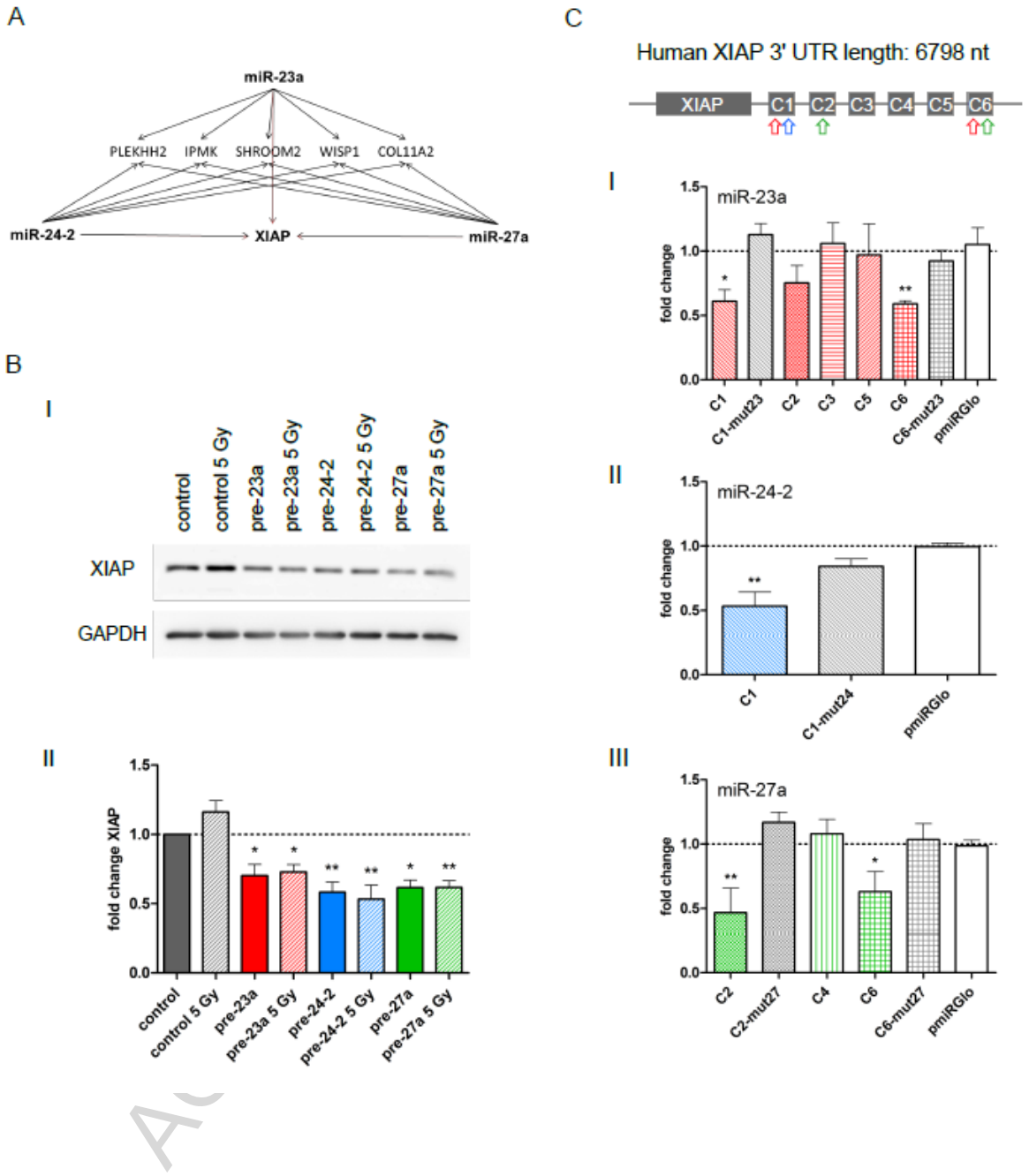

Figure 7

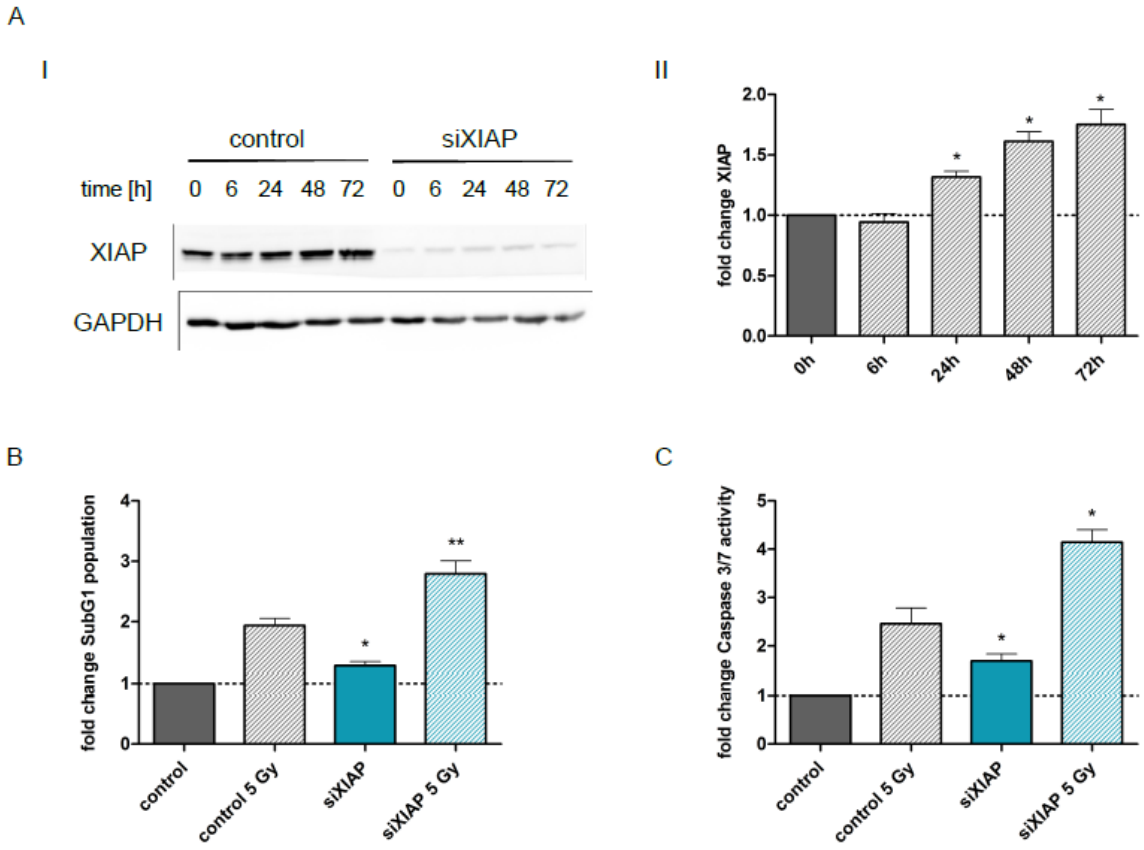

Graphical Abstract

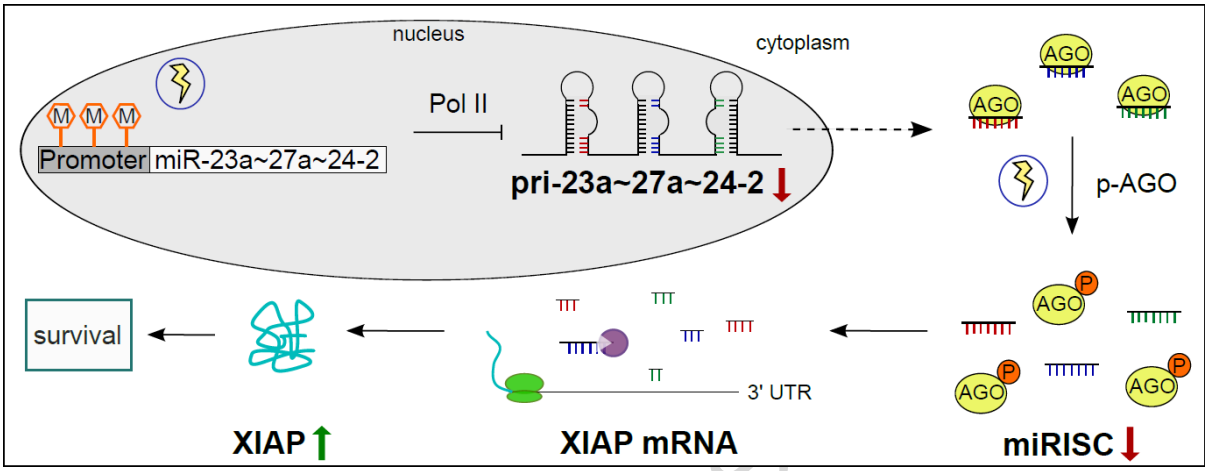

Highlights:

- radiation-induced downregulation of the miR-23a~24-2~27a cluster
- radiation-induced phosphorylation of AGO
- radiation-induced destabilization of cluster miRNAs through reduced AGO binding
- XIAP mRNA is a common direct target of miR-23a, miR-27a and miR-24-2
- cluster downregulation reduces apoptosis through increased XIAP translation